

The Formation of Gypsum Megacrystals

Juan Manuel García-Ruiz^{1*}, Roberto Villasuso², Carles Ayora³,
Angels Canals⁴, Fermín Otálora¹

¹Instituto Andaluz de Ciencias de la Tierra. Consejo Superior de Investigaciones Científicas-
Universidad de Granada, Campus Fuentenueva, E-18002, Granada, Spain

²Compañía Peñoles, Unidad Naica, Naica, Chihuahua, Mexico.

³Institut de Ciències de la Terra Jaume Almera, Consejo Superior de Investigaciones Científicas, Lluís
Solé Sabarís s/n, E-08028 Barcelona, Spain

⁴Dept. de Cristal·lografia, Mineralogia i Dipòsits Minerals, Universitat de Barcelona, Martí Franquès
s/n, E-08028 Barcelona, Spain

* To whom correspondence should be addressed (email: jmgruiz@ugr.es).

Abstract

Exploration activities in the mine of Naica (Chihuahua, Mexico) recently unveiled several caves containing giant, faceted and transparent single crystals of gypsum ($\text{CaSO}_4 \cdot 2\text{H}_2\text{O}$) up to eleven meters in length. Understanding the formation of giant crystals under natural conditions remains one of the mysteries of mineralogy. The problem lies on the impossibility of reproducing the phenomenon at the laboratory time scale and on the absence of a well-known geological framework for most of the cases reported in the literature. Based on geological and geochemical data, fluid inclusions geothermometry and crystallization studies, we claim that these megacrystals formed by a self-feeding mechanism driven by solution mediated anhydrite-gypsum phase transition. The evidences presented show that this mechanism is the only one that can

25 **account for the formation of these giant crystals, and only when operating within a very narrow**
26 **range of temperatures, slightly below the one at which solubility of both phases equals. These**
27 **singular conditions create a mineral wonderland, a site of scientific interest, and an**
28 **extraordinary phenomenon worthy of preservation.**

29

30 **GEOLOGICAL SETTING**

31 The Naica mine is located on the northern side of the *Sierra de Naica*, 112 km SE of Chihuahua city in
32 Northern Mexico and constitutes one of the most important lead and silver deposit in the world.

33 Geologically, the area is dominated by a domian structure oriented NW-SE of 12 km long and 7 km
34 wide standing out from a very extensive alluvial plain. Naica mining district is entirely formed by
35 sedimentary rocks, consisting in a sequence of Albian limestones with some lutitic interbeddings lying
36 upon an evaporitic sequence of Aptian age, which have been found in the regional surroundings but not
37 in the mining district. The sedimentary rocks are intruded by Tertiary acidic dykes dated 26.2 and 25.9
38 millions years old (Megaw *et al.*, 1988). The existence of an igneous source located 4 km south of
39 Naica mine at depth between 2 and 5 km has been revealed by magnetometric studies. The
40 hydrothermal fluid circulation associated to the Tertiary dykes formed the Ag-Pb-Zn deposits (Lang,
41 1995). These deposits—displaying chimney and manto shapes—develop both in the dykes and in the
42 enclosing carbonates, which appear intensively transformed to calcosilicates. The ore assemblage is
43 made up of pyrite-pyrrhotite, sphalerite, galena and chalcopyrite. Late quartz-calcite-anhydrite veins
44 cut the ore (Stone, 1959). Finally, two sets of faults work as the main structural controls of the
45 mineralization, Gibraltar, Montaña and Naica being the most important of them (Fig. 1).

46

47 The Peñoles mining company has excavated galleries down to –760 m from the main access gallery
48 (level 0 at 1385 m a.s.l.). This requires an average pumping of 55 m³/min to create a depression cone of

49 –580 meters with relation to the phreatic level located at -120 meters, Naica and Gibraltar faults acting
50 as the main drains (Fig. 1). The area is still under a thermal anomaly. Water samples collected at
51 different times and mine locations show that the temperature of the groundwater is around 53°C in the
52 deep levels of the mine although temperatures as high as 59°C have been measured (Table DR4). As
53 expected from the lithological setting present waters have low salinity, are rich in calcium, sulfate and
54 carbonate, and according to their isotopic values (Table DR3) they have a meteoric origin with more
55 than 50 years of residence time in the aquifer.

56

57 **GIANT SELENITE CRYSTALS**

58 Since early twentieth century, the excavation of new galleries and tunnels occasionally leads to the
59 discovery of cavities and caves that contain meter-size crystals of selenite, the colorless crystalline
60 variety of gypsum. The caves are always located near fractures and their walls are covered by a red
61 coating made of calcite and celestite with minor amounts of iron oxide, montmorillonite, chlinochlore
62 and illite. The absence of alunite and kaolinite minerals as well as the values of sulfur isotopes discards
63 a sulfuric speleogenesis mechanism (Polyak and Güven, 1996). In 2000, several caves were discovered
64 at level –290 m in secondary faults associated with the Naica fault (Fig. 1). At that depth the impact of
65 oxygen enriched waters is very unlikely and consequently the gypsum crystals contain very few solid
66 inclusions of iron and manganese oxides. One of these caves, named the *Cueva de los Cristales* (Cave
67 of the Crystals), contains selenite crystals up to eleven meters long and one meter thick, i.e., much
68 larger than any gypsum crystal previously reported (Foshag, 1927; García-Guinea *et al.*, 2002; Palache,
69 1932; Rickwood, 1981). The walls of the cave and particularly the floor are sprinkled with blocky
70 single crystals that in some cases cluster to form parallel aggregates (Fig. DR6). Rather than having the
71 characteristic platy or tabular habit of the gypsum crystals, they are euhedral displaying well
72 developed {010}, {1k0} and {-111} (Fig. DR2). The {010} pinacoid is less developed than in the usual
73 growth morphology of gypsum crystals. The {1k0} prismatic form appears as striated surface made of

74 segments of prismatic forms with $k = 2, 4$ or 6 , as shown by laser reflection goniometry and scanning
75 electron microscopy (Fig. DR3, DR4 and Table DR1). The resulting non singular face has an
76 orientation close to $\{140\}$. The unusual blocky habit, the development of the more acute prismatic
77 faces $\{140\}$ and $\{160\}$ instead of the usual $\{120\}$ (Simon and Bienfait, 1965) and the alignment of the
78 crystals with the edge $[010]$ vertical, give them an impressive and intimidating sharktooth appearance
79 (Fig. 2 and DR6). From some of these groups of blocky crystals or directly from the floor, grow
80 elongated giant selenite crystals, some of which cross the cave from side to side. Most of these crystals
81 are six meters long and several of them reach ten meters. Consequently, the miners correctly term them
82 *vigas* (beams), not swords. There is only one morphological difference between the beams and the
83 blocky crystals, namely that the pinacoidal cleavage faces $\{010\}$ disappear in most cases. The
84 crystalline beams are elongated along the zone axis c , defined by huge prismatic $\{1k0\}$ faces capped by
85 the $\{-111\}$ prism (Fig. DR5). Finally what makes this a natural scenario of unparallel beauty—and it is
86 critical to explain its formation—is the small number of crystals (Fig. 2) that can only result from
87 extremely low nucleation rates: therefore the value of the driving force for crystal nucleation was kept
88 small (close to equilibrium) for the entire history of the system.

89

90 **GEOCHEMICAL CONDITIONS**

91 We have measured ice melting temperatures from 33 selected fluid inclusions which were biphasic at
92 room temperature (Fig. DR9 and Table DR2). The range of obtained temperatures indicates low
93 salinity values compatible with today meteoric and mine waters (Bodnar, 1993; Bakker, 2003). That
94 means that the original high-salinity sulfur rich acidic magmatic fluids (Lang, 1995; Erwood *et al.*,
95 1979) that provoked the skarn formation had practically lost the salinity at the time the gypsum crystals
96 grew. Sulfuric acid formed by oxidation of underlying sulfides deposit reacted with limestone to form
97 calcium sulfate rich waters that precipitated the stable polymorph (anhydrite) during the late

98 hydrothermal stage. In fact, anhydrite appears massively in Naica at any level below 240 meters.
99 Cooling of the system and contribution of meteoric waters yield sulfate and carbonate rich water with a
100 temperature in the range of 48-59°C, and a neutral to slightly basic pH (7.0-7.8), like the one today
101 gushed out of the mine. As shown in Fig. 3, the isotopic values of these gypsum crystals are consistent
102 with their formation from waters with dissolved sulfate similar to those found in present day
103 groundwater collected at level -530 (Fig. 3b). The isotopic values of sulfate dissolved in the water can
104 be explained by mixture of sulfates from the dissolution of anhydrite from different locations of the
105 mine, those from the ore deposit area (samples 23, 24, 25 and 34) and those from upper levels in the
106 mine (sample 04 and 21 in Table DR3). This is also confirmed by the presence of celestite, a strontium
107 sulfate found together with clays and iron oxide in a thin layer coating the walls of the Cave of the
108 Crystals. It has been demonstrated that anhydrite structure hosts more strontium than gypsum
109 (Butler, 1973); celestite crystals resulted from the excess of strontium hosted in the dissolving
110 anhydrite with respect to crystallizing gypsum (See table DR4). These data discards the
111 hypothesis of mixing of water of different salinity as the source for the driving force for crystallization
112 and suggest a mechanism for the formation of gypsum crystals based upon Ostwald's law of phase
113 stability.

114

115 **FORMATION OF MEGACRYSTALS**

116 Gypsum is slightly soluble in water ($13.78 \cdot 10^{-3} \text{ mol L}^{-1}$ at 25°C and atmospheric pressure) (Partridge
117 and White, 1929). Its solubility shows a positive dependence on temperature in cool waters, reaching a
118 maximum at about 58°C and then decreasing until 107°C where the solubility is minimum because of
119 the formation of the hemihydrate (Posnjak, 1938). The solubility of gypsum also has a positive
120 variation with salinity but the temperature of maximum solubility does not change significantly,

121 keeping close to 58°C. At atmospheric pressure, gypsum becomes unstable at temperatures hotter than
122 56-58°C (Hardie, 1967; Blount and Dickson, 1973) while anhydrite becomes unstable with respect to
123 gypsum at temperatures lower than 58°C (Fig. 4a). Therefore, upon cooling of the Naica district,
124 hydrothermal anhydrite associate to the late stage of the formation of the ore deposit became unstable
125 and is dissolved, thus explaining the high content of sulfate anions in the present day waters. The
126 dissolution of anhydrite below 58°C supplies Ca²⁺ and SO₄²⁻ to keep the water slightly supersaturated in
127 gypsum and promoting its precipitation. Examples of this replacement are also observed at microscopic
128 scale in some anhydrite masses close to the cave of the crystals (See Fig. DR11). Actually,
129 supersaturation values ($S = c/c_e$ where c is the actual concentration and c_e is the equilibrium
130 concentration for a given temperature and salinity) calculated for present day waters yields values
131 slightly supersaturated for gypsum and undersaturated for anhydrite. Such a small difference between
132 the solubility of gypsum and anhydrite slightly below 58°C is a continuous source of calcium and
133 sulfate molecules and also a very stable mechanism to constantly maintain the precipitation system
134 close to equilibrium. The question is how much cooling the system may have undergone to avoid the
135 massive nucleation that would have packed the caves with a large number of small crystals. The
136 nucleation flux is described by the equation:

137
$$J = A \exp - \frac{16 \pi \gamma^3 v^2}{3k^3 T^3 \ln^2 S}$$

138 Where γ is the crystal/liquid interfacial tension, v is the molecular volume, k is the Boltzman constant,
139 and T is the absolute temperature. As the nucleation flux J varies with the second power of the
140 logarithm of supersaturation S , low values of J means that supersaturation was kept in the metastable
141 zone and very close to equilibrium for the whole history of crystallization in the cave. The induction
142 time t_{ind} or waiting time for nucleation being inversely proportional to J , the above equation can be
143 written as a linear relationship:

144
145
146
147
148
149
150
151
152
153
154
155
156
157
158
159
160
161
162
163
164
165
166
167

$$\log t_{ind} \propto \frac{\gamma^3}{T^3 \log^2 S}$$

Using experimental data available from gypsum nucleation studies (He *et al.*, 1994; Lancia *et al.*, 1999) we have calculated (for both, homogeneous and heterogeneous nucleation) the induction time for three salinities: just calcium, sulfate and water molecules (labeled 0), salinity values (Na, Cl and Mg concentration) identical to those found in Naica waters (labeled 1) and twice these concentrations (labeled 2) (Fig. 4b). For any large geological reservoir where crystallization occurs, heterogeneous nucleation is unavoidable because it requires lower critical supersaturation values to surpass the nucleation barrier. As shown in Figure 4b, the waiting time for heterogeneous nucleation becomes in the order of thousands of years for temperatures of 47-48°C. For any temperature below 44-45°C we found a very large probability for a nucleation event in the scale of months or days, which cannot explain the small number of crystals in the caves. We have measured homogenization temperatures (T_h) of 31 fluid inclusions; the data show a distribution with a maximum around 54±1°C (Fig. 4c, Table DR2). Accordingly with the proposed mechanism, this value indicates that most of the crystallization process took place at a temperature for which t_{ind} is longer than a million years (Fig. 4b). These close to equilibrium conditions were maintained for a long time with some episodes of cessation of growth, as suggested by the occasional solid inclusions of manganese and iron oxi-hydroxides on {1k0} and {-111} growth fronts. Eventually, as indicated by lower values of T_h down to 47°C, the system cooled down due to a stronger influence of meteoric waters and the probability of nucleation was higher, in the order of thousand of years. Accordingly, with this mechanism, caves such as the Cave of the Swords (Foshag, 1927) that are located closer to the surface undergo lower temperatures and are filled with large number of smaller crystals (Fig. 1 and Fig. DR1).

The gypsum crystals of Naica are the result of a natural experiment irreproducible at laboratory time scale. Interestingly, these crystals supply information demonstrating the current lack of understanding

168 of equilibrium crystal morphology, which particularly in the case of gypsum is a long standing problem
169 (Simon and Bienfait, 1965; Weijnen *et al.*, 1987, Heijnen and Hartman, 1991). The morphology of long
170 beams showing the preferential development of non singular $\{1k0\}$ faces in relation to the cleavage
171 face $\{010\}$ suggests that ordering at the hydration layer is at least as important as bonding
172 configuration in the three-dimensional structure, a hypothesis suggested by van der Voort and Hartman
173 (1991).

174

175 It can be predicted that other caves with similar or even larger selenite crystals can be unseen among
176 the tangle of underground roads drawn in Naica mine for exploration and management of ore minerals.
177 Together they may constitute one of the oddest locations of the mineral world and are worthy of
178 preservation as a geological marvel. Two problems can be envisaged for that task. The cave must be
179 kept wet and hot but equally important is the development of a method to maintain the integrity of the
180 long *vigas* that bend and break once the buoyancy support of the cave water was lost. The second
181 problem is in the long term but more critical: as soon as the mining work is completed, water pumping
182 will stop and the caves will be again flooded to their natural state. According to the proposed
183 mechanism, the selenite crystals will start to grow again but they will be hidden for future generations.
184

185 **Acknowledgements**

186 We gratefully acknowledge Compañía Peñoles for the facilities provided during the field studies
187 performed in Naica mine. Ministerio de Educación y Ciencia of Spain is acknowledged for financial
188 support offered at the final stage of this study.

189

190 **Figure Captions**

191 **Figure 1:** Geological section of the Naica mine. The mine works a hydrothermal Pb-Zn-Ag deposit
192 with irregular ‘manto’ and ‘pipe’ morphologies entirely enclosed in carbonates (not represented for

193 simplicity). The cavities of gypsum crystals are located in the carbonates close to main and secondary
194 faults. Original and current water level are shown.

195

196 **Figure 2:** A view of the Cave of Crystals showing the characteristic moonlight lustre that name (Selene
197 is the Greek name for the moon) these gypsum crystals. Two crystal morphologies can be observed, the
198 blocky crystals displaying the prisms $\{1k0\}$ and $\{-111\}$ and the pinacoid $\{010\}$ and the beams, which
199 are crystals elongated along the c axis displaying only the prismatic crystal faces. Notice that the
200 population of crystals is much lower in the ceiling of the cave than on the floor. For very large waiting
201 time for nucleation, this gradation is due to a density layering of the solution filling the cave (Turner,
202 1985), which increases the probability of nucleation from the solution located in the lower part of the
203 cavern.

204

205 **Figure 3:** Isotope composition of the sulfate molecules in gypsum, anhydrite and water collected at
206 Naica mine. The polygonal surface envelopes the isotope composition of the water from which the
207 gypsum crystals grew.

208

209 **Figure 4:** a) Variation of anhydrite and gypsum solubility with temperature for three different values of
210 salinity: (0) for pure calcium sulphate solutions; (1) for salinity equal and (2) twice the one found in
211 current water collected at Naica mine. Solubility calculated with PHREEQC (Parkhurst, 1980) using
212 the PHREEQC database. b) Waiting time for (homogeneous and heterogeneous) nucleation calculated
213 for supersaturated solutions forming by differences in solubility between anhydrite and gypsum at
214 different temperatures. c) Homogenization temperatures of 31 fluid inclusions showing the actual
215 temperature of growth. The heating rate was of $2^{\circ}\text{C}/\text{min}$, and the precision of the measurement is
216 estimated to be $\pm 1^{\circ}\text{C}$. From the geological setting no correction due to confinement pressure is
217 required, and this temperature range can be considered the actual temperature of crystal growth.

219 **References cited**

- 220 • Bakker, R.J., 2003, Package FLUIDS 1. New computer programs for the analysis of fluid
221 inclusion data and for modelling bulk fluid properties: *Chemical Geology*, v. 194, p. 3-
222 23.
- 223 • Blount, C.W. and Dickson, F.W., 1973, Gypsum-anhydrite equilibria in systems CaSO₄-H₂O
224 and CaSO₄-NaCl-H₂O: *American Mineralogist*, v. 58, p. 323-331.
- 225 • Bodnar, R. J., 1993, Revised equation and table for determining the freezing point depression of
226 H₂O-NaCl solutions: *Geochimica Cosmochimica Acta*, v. 57, p. 683-684
- 227 • Butler, G.P., 1973, Strontium geochemistry of modern and ancient calcium sulphate minerals,
228 in Purser, B.H., ed., *The Persian Gulf*: Springer-Verlag, Berlin Heidelberg New York, p. 423-
229 452.
- 230 • Erwood, R.J., Kesler, S.E., and Cloke, P.L., 1979, Compositionally distinct, saline
231 hydrothermal solutions, Naica Mine, Chihuahua, Mexico: *Economic Geology*, v. 74, p. 95-108.
- 232 • Foshag, W., 1927, The selenite caves of Naica, Mexico: *American Mineralogist*, v. 12, p. 252-
233 256.
- 234 • García-Guinea, J., Morales, S., Delgado, A., Recio, C., and Calahorra, J.M., 2002, Formation of
235 gigantic gypsum crystals: *Journal of the Geological Society*, v. 159, p. 347-350.
- 236 • Hardie, L.A., 1967, The gypsum-anhydrite equilibrium at one atmosphere pressure: *American*
237 *Mineralogist*, v. 52, p. 171-200.
- 238 • He, S., Oddo, J. E., and Tomson, M.B., 1994, The Nucleation Kinetics of Calcium Sulfate
239 Dihydrate in NaCl Solutions up to 6 *m* and 90°C: *Journal of Colloid and Interface Science*, v.
240 162, p. 297-303.
- 241 • Heijnen, W.M.M. and Hartman, P., 1991, Structural morphology of gypsum (CaSO₄·2H₂O),

- 242 brushite ($\text{CaHPO}_4 \cdot 2\text{H}_2\text{O}$) and pharmacolite ($\text{CaHAsO}_4 \cdot 2\text{H}_2\text{O}$): *Journal of Crystal Growth*, v.
243 108, p. 290-300.
- 244 • Lancia A., Musmarra D., Prisciandaro M., 1999, Measurement of the induction period for
245 calcium sulfate dihydrate precipitation: *AIChE Journal*, v. 45, p. 390-397.
 - 246 • Lang, J.R., 1995, A geological evaluation of the Naica deposit, Chihuahua, Mexico: Internal
247 Report of Compañía Fresnillo. 109 pp.
 - 248 • Megaw, P.K.M., Ruiz, J., and Titley, S.R., 1988, High-temperature, carbonate-hosted Pb-Zn-Ag
249 (Cu) deposits of northern Mexico: *Economic Geology*, v. 83, p. 1856-1885.
 - 250 • Palache, Ch., 1932, The largest crystal: *American Mineralogist*, v. 17, p. 362-363.
 - 251 • Parkhurst, D.L., Thorstenson, D.C. and Plummer, L. N., 1980, PHREEQE-A Computer
252 Program for Geochemical Calculations: *Water Resources Investigations* 80-96. Reston,
253 Virginia, U.S. Geological Survey: 210 p.
 - 254 • Partridge, E.P. and White, A.H., 1929, The solubility of calcium sulfate from 0 to 200°: *Journal*
255 *of the American Chemical Society*, v. 51, p. 360-370.
 - 256 • Polyak, V.J. and Güven, N., 1996, Alunite, natroalunite and hydrated halloysite in Carlsbad
257 Cavern and Lechuguilla Cave, New Mexico: *Clays and Clay Minerals*, v. 44, 843-850.
 - 258 • Posnjak, E., 1938, The system $\text{CaSO}_4\text{-H}_2\text{O}$: *American Journal of Science*, v. 235A, p. 247-272.
 - 259 • Rickwood, P.C., 1981, The largest crystals: *American Mineralogist*, v. 66, p. 885-907.
 - 260 • Simon, B. and Bienfait, M., 1965, Structure et mécanisme de croissance du gypse: *Acta*
261 *Crystallographica*, v. 19, p. 750-756.
 - 262 • Stone, J.G., 1959, Ore genesis in the Naica District, Chihuahua, Mexico: *Economic Geology*,
263 v. 54, p. 1002-1034.
 - 264 • Turner, J.S., 1985, Multicomponent convection: *Annual Review of Fluid Mechanics*, v. 17, p.
265 11-44.
 - 266 • van der Voort, E., Hartman, P., 1991, The habit of gypsum and solvent interaction: *Journal of*

267 Crystal Growth, v. 112, p. 445-450.

- 268 • Weijnen, M.P.C., van Rosmalen, G.M., Bennema, P. and Rijpkema, J.J.M., 1987, The
269 adsorption of additives at the gypsum crystal surface: A theoretical approach : I.
270 Determination of the interfacial bond energies: Journal of Crystal Growth, v. 82, p. 509-
271 527.

272

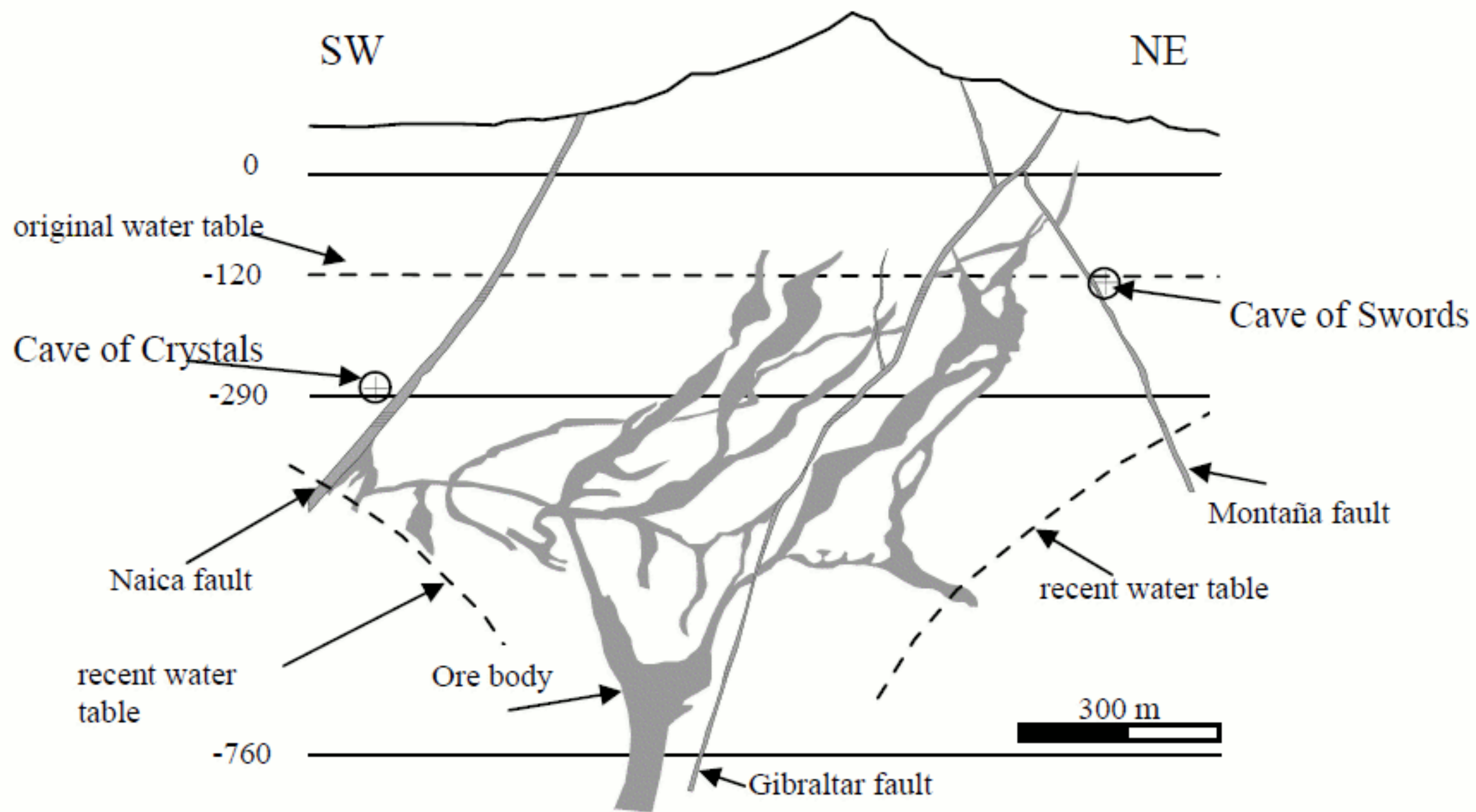


Fig. 1. García-Ruiz, Villasuso, Ayora, Canals & Otálora. (GIF)



Fig. 2. García-Ruiz, Villasuso, Ayora, Canals & Otalora (GIF)

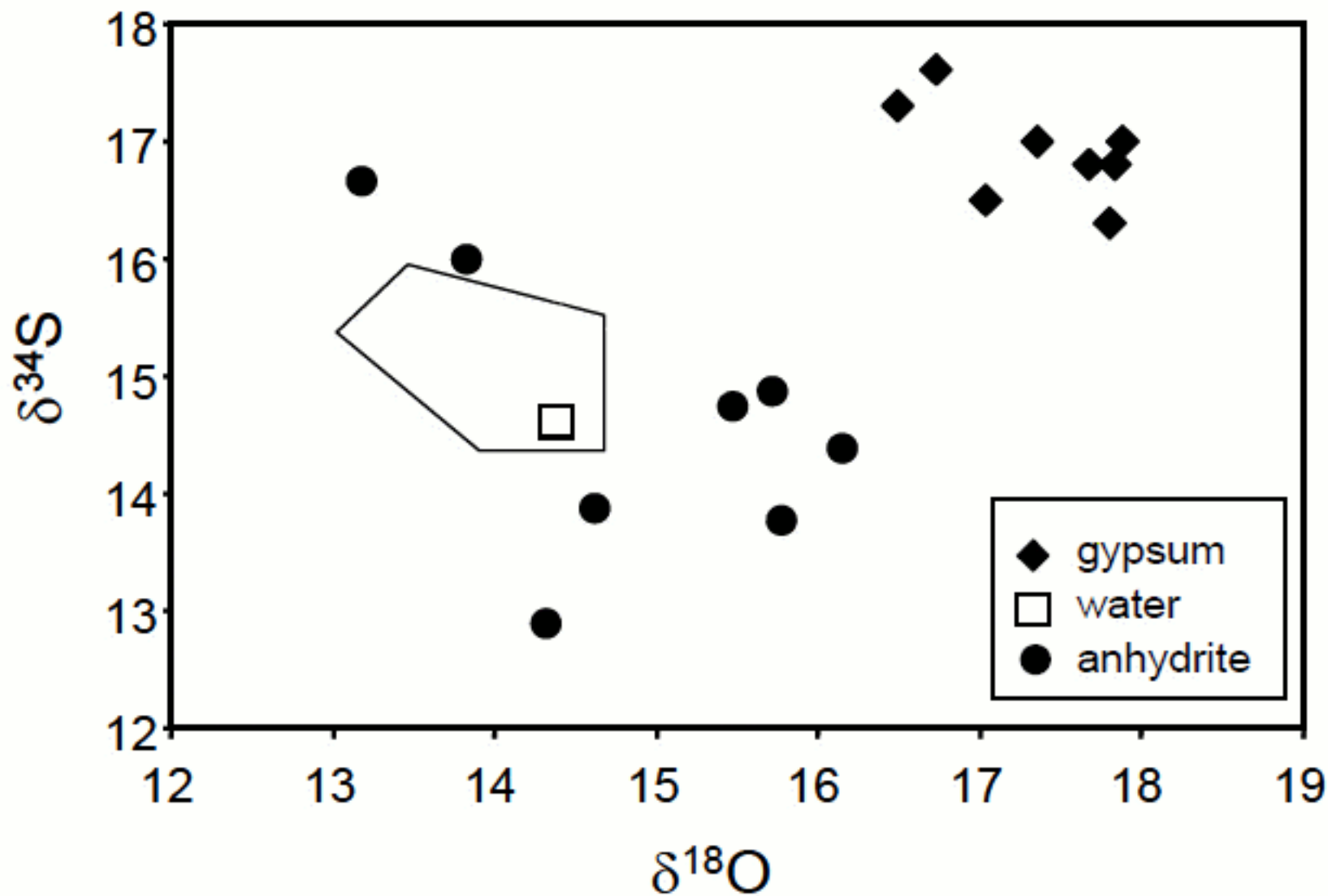


Fig. 3. García-Ruiz, Villasuso, Ayora, Canals & Otálora. (GIF)

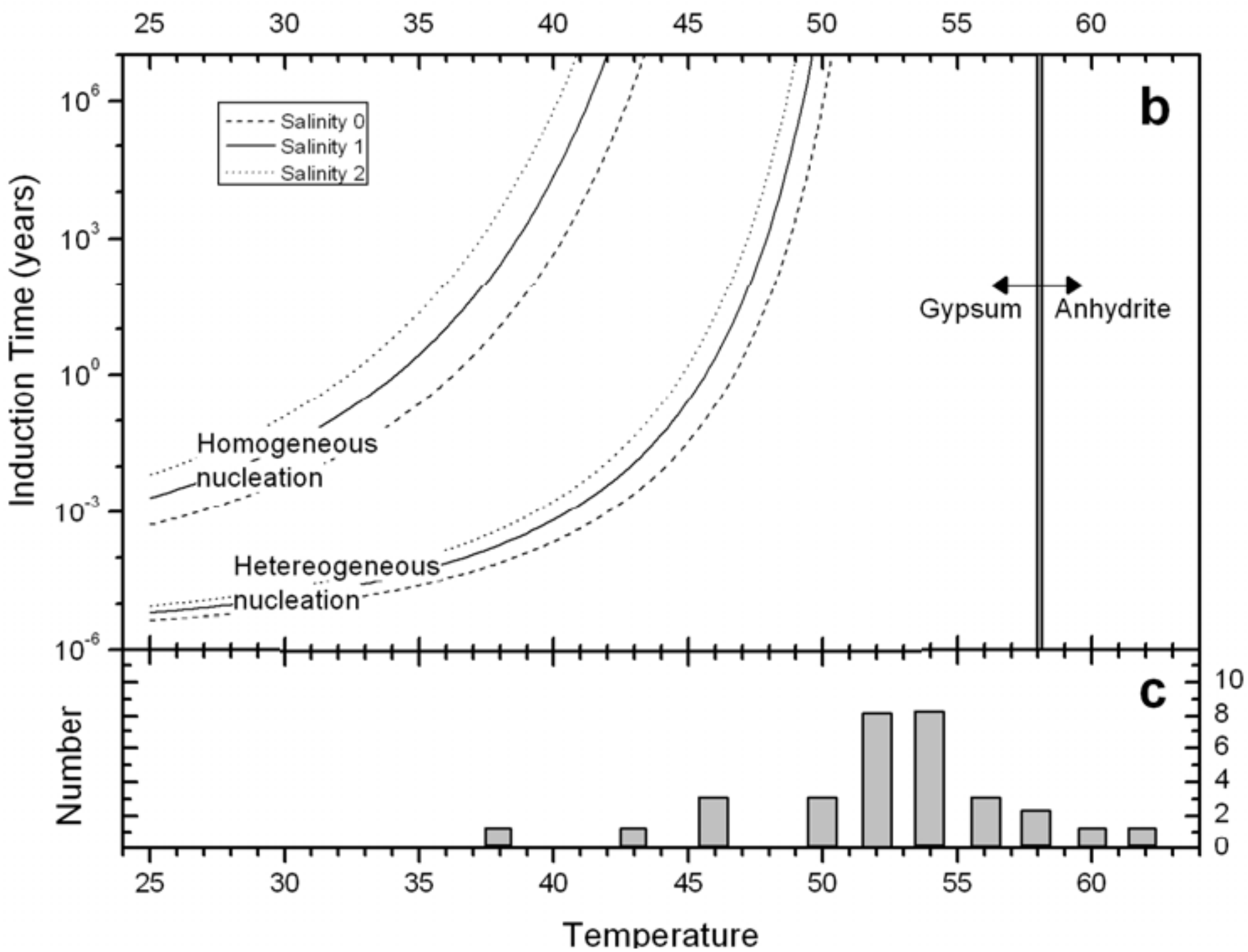
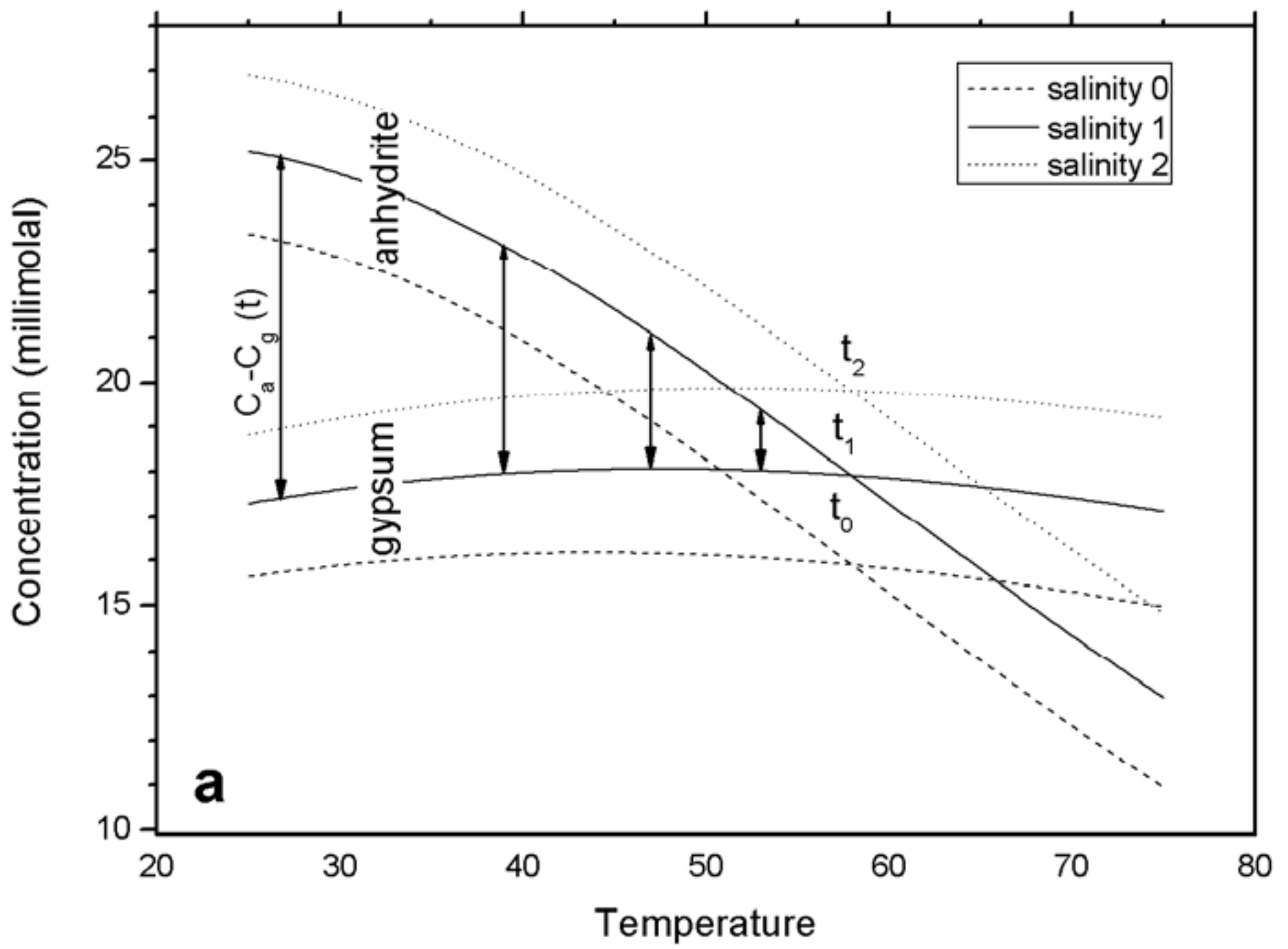


Fig. 4. García-Ruiz, Villasuso, Ayora, Canals & Otálora. (GIF)